Earth-Science Reviews 212 (2021) 103451

Contents lists available at ScienceDirect

Earth-Science Reviews

journal homepage: www.elsevier.com/locate/earscirev

Understanding interactions among climate, water, and vegetation with the Budyko framework

Guojing Gan [a,b], Yuanbo Liu [a,*], Ge Sun [c]

[a] Nanjing Institute of Geography and Limnology, Chinese Academy of Sciences, Nanjing, China
[b] Key Laboratory of Watershed Geographic Sciences, Chinese Academy of Sciences, Nanjing 210008, China
[c] U.S. Department of Agriculture, Forest Service, Southern Research Station, Eastern Forest Environmental Threat Assessment Center, Research Triangle Park, NC 27709, USA

ARTICLE INFO

Keywords:
Budyko model
Vegetation effect
Catchment water balance
Climate-vegetation interaction

ABSTRACT

The Budyko models provide a transparent framework for analyzing climate-catchment interactions and therefore have been widely used to quantify the role of vegetation influencing the partitioning of precipitation (P) into evapotranspiration (ET) and runoff (R) at watershed to regional scales under a changing environment. This study provides a thorough review of the use of Budyko models for answering modern hydrological questions including the relation between vegetation dynamic and catchment ET (or runoff) and climate change impacts on water balances. Our synthesis suggests that:

When vegetation structure and rooting characteristics are included, the Budyko models can explain over 90% of global spatial variations in ET. Budyko models showed that although climate dominates the catchment water balance, forest cover change also accounts for 30.7% ± 22.5% change in annual runoff in watersheds globally. Vegetation in watersheds with a low water retention capacity tends to play a more important role than climate change. Vegetation effects on annual runoff are most pronounced in water-limited regions and large scale revegetation can contribute 60% of the total observed change in the annual runoff. Budyko models can be used to study the joint impacts of climate seasonality (rainfall frequency and the time lag between maximum precipitation and net radiation) and vegetation on interannual variations in water balances.

We conclude that vegetation dynamics have been successfully incorporated into the Budyko framework in the past two decades. The Budyko framework can be extended to provide insights into the interactions between climate, hydrology, and ecology. Uses of the Budyko framework for studying the hydrological effects of vegetation dynamics under a changing climate require analytical derivations of the models that incorporate climate-vegetation coevolution procedures.

1. Introduction

Quantifying factors that control the partitioning of atmospheric precipitation into runoff (R), evapotranspiration (ET), and water storage at a watershed scale is the most fundamental pursuit in hydrology. Intuitively, because ET refers to the water phase transition from liquid to vapor, the evaporation rate is mainly controlled by the water-energy balance on the evaporating surface (Williams et al., 2012). Therefore, land surface ET and runoff are the competing outcomes of water supply (precipitation, P) and demand (net radiation, R_n, or potential ET, ET_0) from the atmosphere. Based on the "Supply-demand" balance, Budyko (1974) estimated long-term (> > 1 year) ET of a catchment using climate dryness (φ, $\varphi = R_n/P$) with a universal non-dimensional curve, which is now known as the Budyko curve (Eq. (1)).

$$\frac{ET}{P} = \left[\frac{R_n}{P}\tanh\left(\frac{R_n}{P}\right)^{-1}\left(1 - exp\left(-\frac{R_n}{P}\right)\right)\right]^{0.5} \quad (1)$$

Besides climate conditions (P and ET_0), ET and R are also greatly affected by the terrestrial ecological processes, especially the vegetation dynamics (Murray et al., 2012; Sun et al., 2015; Sun and Vose, 2016; Woodward et al., 2014). For example, the existence of vegetation alters the humidity conditions of the land surface by intercepting the rainfall and retaining water through its roots (Guswa, 2008), which will have great impacts on annual and intra-annual variation in ET and runoff

* Corresponding author.
E-mail address: ybliu@niglas.ac.cn (Y. Liu).

https://doi.org/10.1016/j.earscirev.2020.103451
Received 20 December 2019; Received in revised form 8 October 2020; Accepted 22 November 2020
Available online 25 November 2020

because plants usually experience substantial variations at interannual and decadal time scales (Arora, 2002; Porporato et al., 2004). Furthermore, plants can adapt to different climate conditions (Gentine et al., 2012; Helman et al., 2017; Troch et al., 2013), which will feed back to the water balance of a watershed. For example, the rooting depth of the plant tends to increase with the phase lag between P and ET_0 (Schenk and Jackson, 2002), and annual ET would be smaller without plant adaptation if precipitation and radiation are out-of-phase (Feng et al., 2012).

Global vegetation has experienced tremendous changes during the last several decades (Chen et al., 2019; Zhu et al., 2016). Vegetation greening has occurred in the high Arctic (Vickers et al., 2016), northern regions in Europe-Asia, north America (Park et al., 2016), in developing countries (especially in China and Indian) (Chen et al., 2019) due to the large scale plantation, and global drylands (under natural conditions), caused by increasing atmospheric CO_2 concentration (Donohue et al., 2013; Donohue et al., 2017). Vegetation losses are also reported in many regions, e.g., southwestern Amazon (Lima et al., 2014) and large lake basins of America (Mao and Cherkauer, 2009). Although it is widely accepted that the existence of vegetation (especially forests) have positive effects on increasing ecosystem carbon sequestration and reducing soil erosion, afforestation may exert negative impacts on water resources by reducing the water yield of catchments (Feng et al., 2012; Zhang et al., 2018b). For example, in China, afforestation has the potential to reduce streamflow by 50–150 mm/y or 20–40% across most of the nation (Sun et al., 2006). Reviews on hydrological responses to forest change in small watersheds have concluded that afforestation decreases streamflow (Beck et al., 2013; Bi et al., 2009; Brown et al., 2005; Stednick, 1996). However, no consensus has been reached for large watersheds (Hibbert, 1967; Kokkonen and Jakeman, 2001; Zhang et al., 2017), although urge needs to include vegetation changes into global water assessments have been clearly recognized (Arnell and Gosling, 2013; Schewe et al., 2014).

To study the vegetation effect on the variations and trends in catchment ET and runoff, the Budyko-type models (Andreassian and Perrin, 2012; Donohue et al., 2007; Sposito, 2017; Wang et al., 2016) were intensively used in recent decades (Li et al., 2013; Xu et al., 2013), e.g., in United States (Wang and Hejazi, 2011), Australia (Donohue et al., 2012), China (Xing et al., 2018a), and European regions (Oudin et al., 2008), providing insights from the water-energy balance perspectives. Unlike the process-based models that usually need large numbers of parameters (Lei et al., 2014; Shen et al., 2013), the Budyko-type models belong to the top-down approaches (Sivapalan et al., 2003; Wang and Tang, 2014), whose complexity is increased only when the existing factors are insufficient to explain the observed changes (Zhang et al., 2008a). Therefore, Budyko-type models are often concise and can provide transparent analysis on the climate-catchment interactions (Gao et al., 2016a; Liang et al., 2015; Monserud et al., 1993; Warren and Schneider, 1979). Using the Budyko-type models, the relative contribution of climate (Koster and Suarez, 1999; Xing et al., 2018c), water storage (Chen et al., 2013; Wang, 2012; Zeng and Cai, 2015; Zeng and Cai, 2016), and human activities including vegetation changes (Li et al., 2018; Li et al., 2012) to the variances and trends of catchment water balance can be derived in an analytical and transparent way.

In this paper, we gave a thorough review of the vegetation effect on catchment water balance within the Budyko framework. We summarized how the original Budyko models were extended to incorporate the dynamic information of vegetation characteristics (Section 3) and quantify the respective contribution of vegetation change and climate change on water balance trends (Section 4). We then discuss climate-vegetation interactions within the Budyko framework under different climate conditions (Section 5), and limitations of the models in Section 6. Conclusion and prospects were summarized in Section 7.

2. Budyko's perspective: climate control on catchment water balance

Climate characteristics (P and ET_0) determines catchment water balance at long time scales (Ol'Dekop, 1911; Pike, 1964; Turc, 1954). Date back to the early 20th century, the multi-year runoff coefficient (R/P) was found to increase with precipitation (Schreiber, 1904), as shown in Eq. 2, where a_{sch} is a positive parameter. Ol'Dekop (1911) further found that a_{sch} can be replaced by an atmospheric "demanding" term for water, which exerts a negative effect on water yield, as shown in Eq. 3.

Therefore, the "supply-demand" competition serves as the determinant control on ET and runoff (Budyko, 1974): 1) when $R_n/P \to \infty$ (extremely dry), $ET/P \to 1$, indicating that all precipitation is used for evaporation and water is the limiting factor for ET; 2) when $R_n/P \to 0$ (extremely humid), $ET/R_n \to 1$, indicating that all energy is used for evaporation and energy is the limiting factor for ET. Following the above two hypotheses, Budyko (1974) derived a simple curve (Eq. 5, Fig. 1) to describe the universal relationship between long term ($>>1$ year) ET and climatic forcing. Actual ET takes up a larger proportion in P as climate dryness increases (Fig. 1). Note that net radiation is usually surrogated by ET_0 nowadays, therefore, we use ET_0 instead of R_n in the rest of the paper although R_n was used originally in some of the formulations (Budyko, 1974; Choudhury, 1999; Schreiber, 1904). ET_0 can be estimated using the pan evaporation, the Priestley-Taylor equation (Priestley and Taylor, 1972), and the Penman approach (Penman, 1948).

The Budyko-type formulations that satisfy the two limiting conditions in Budyko's hypothesis are summarized in Table 1. All formulations share some similarities. For example, Budyko (1974)'s formula was derived by geometrically averaging the formulas of Schreiber (1904) and Ol'Dekop (1911), and the Turc-Pike formula (Pike, 1964; Turc, 1954) is a special case of Choudhury (1999) when n is taken as 2. Early empirical formulations (Budyko, 1974; Ol'Dekop, 1911; Pike, 1964; Turc, 1954) represent the overall hydrological responses of catchments to the climatic forcing across the globe because they were derived from continental or global streamflow data. To incorporate the impact of the underlying surface on catchment water balance, Fu (1981) used the dimensional analysis technique and the π theorem to add extra freedom (ω) into the model derivation (Eq. 6, Fig. 1 A) (Zhang et al., 2004). The parameter ω comprehensively reflects the nature of the underlying surface in controlling the allocation of precipitation into R and ET (Rodriguez-Iturbe, 2000). Under the given climate dryness condition, ET takes up a larger proportion of precipitation as ω increases (Fig. 1). Similarly, another one-parameter theoretical equation (Eq. 7) was derived later (Yang et al., 2008), which is consistent with Fu's model and the empirical formula summarized by Choudhury (1999). The consistency of theory and experience increases the credibility of the model. Among all the Budyko-type models, the equations of Fu and Choudhury-Yang are the most commonly used. Particularly, a $\omega = n + 0.72$ relationship exists, because both parameters are correlated with watershed characteristics, including slope, soil texture, and vegetation indices, etc., (Xu et al., 2013; Yang et al., 2009).

Besides the magnitudes of P and ET_0, seasonality of climate forcing also exerts great impacts on the annual water balance of a catchment (Yokoo et al., 2008). For example, with a given amount of annual rainfall, the annual ET of a catchment where rain falls frequently in small amounts may be quite different from the case where the rain falls mainly in a few storms. The hydrological impacts of rainfall seasonality can be incorporated into the Budyko framework by stochastic analysis (Gerrits et al., 2009; Milly, 1993; Porporato et al., 2004). For example, Milly (1993) analytically solved the evaporation index (ET/P) from a stochastic water balance model under the assumption that storm arrivals are Poisson-distributed and storm depth follows an exponential distribution. ET/P is expressed as in Eq. (8) (Milly, 1993), where γ is the ratio of soil water-holding capacity to mean storm depth. With larger γ, ET takes up a larger proportion in precipitation because uniform rainfall

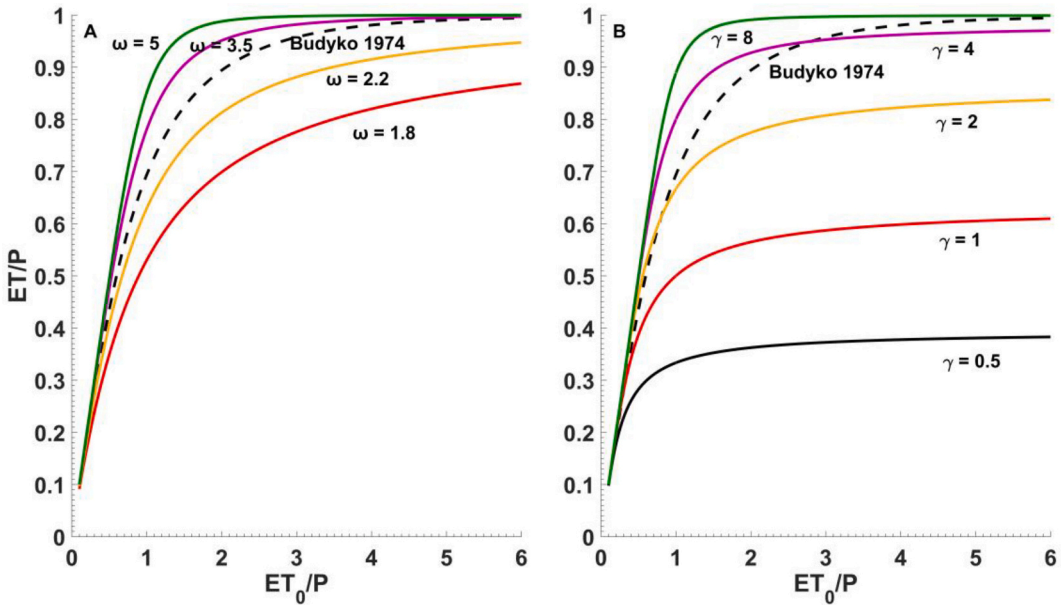

Fig. 1. Budyko-type curves, using (A) The original Budyko equation and Fu's equation when ω was taken as 1.8, 2.2, 3.5, and 5 (from bottom to top), respectively; (B) Milly's equation when γ was taken as 0.5, 1, 2, 4, and 8 (from bottom to top), respectively. The default Budyko-curve (Budyko, 1974) corresponds to a *n* value of 1.9 and a ω value of 2.6.

Table 1
Formulations of the Budyko-type models.

Reference	Formulation
Schreiber (1904)	$\frac{R}{P}=exp\left(-\frac{a_{sch}}{P}\right);\ \frac{ET}{P}=1-exp\left(-\frac{a_{sch}}{P}\right)$ (2)
Ol'Dekop (1911)	$\frac{ET}{P}=\frac{ET_0}{P}tanh\left(\frac{P}{ET_0}\right)$ (3)
Turc (1954); Pike (1964)	$\frac{ET}{P}=\frac{1}{\sqrt{1+(P/ET_0)^2}}$ (4)
Budyko (1974)	$\frac{ET}{P}=\left[\frac{ET_0}{P}tanh\left(\frac{ET_0}{P}\right)^{-1}\left(1-exp\left(-\frac{ET_0}{P}\right)\right)\right]^{0.5}$ (5)
Fu (1981)	$\frac{ET}{P}=1+\frac{ET_0}{P}-\left[1+\left(\frac{ET_0}{P}\right)^{\omega}\right]^{1/\omega}$ (6)
Choudhury (1999); Yang et al. (2008)	$\frac{ET}{P}=\frac{1}{\left[1+(P/ET_0)^n\right]^{1/n}}$ (7)

and/or large water-holding capacity of the catchment favors ET (Fig. 1).

$$\frac{ET}{P}=\frac{exp[\gamma(1-P/ET_0)]-1}{exp[\gamma(1-P/ET_0)]-P/ET_0} \tag{8}$$

$$\frac{ET}{P}=1-\frac{\frac{ET_0}{P}\gamma^{\frac{P}{ET_0}-1}exp^{-\gamma}}{\Gamma\left(\gamma\frac{P}{ET_0}\right)-\Gamma\left(\gamma\frac{P}{ET_0},\gamma\right)} \tag{9}$$

In Milly (1993), evaporation was assumed to occur at its potential rate during the intervals of rainfall events. To obtain more realistic results, Porporato et al. (2004) modeled ET as a function of soil moisture and derived the ET/P expression using Budyko's dryness index and the seasonality of precipitation, as shown in Eq. (9), where r is the Gamma function.

In summary, the Budyko framework characterizes the controls of climate and its seasonality on water balance in an analytical and transparent way. The impacts of catchment properties are comprehensively reflected by the shape parameters of the Budyko curves, such as ω in Fu's equation (Fu, 1981), *n* in Choudhury-Yang equation (Choudhury, 1999; Yang et al., 2008), and γ in the equations of Milly (1993) and Porporato et al. (2004). However, because only vegetation exhibits obvious seasonal and inter-annual changes among the land surface properties (Roderick and Farquhar, 2011), and more importantly because the vegetation can adapt to the changing climate (P, ET_0 and their seasonality) and feed back to the water balance at a decadal time scale (Gentine et al., 2012; Troch et al., 2015), the vegetation effect on the water balance becomes a very crucial issue for understanding the hydrological process of catchments.

3. Vegetation effects on interannual water balance within the Budyko framework

In the recent two decades, the Budyko framework was extended to incorporate vegetation dynamics to 1) capture the variances in annual ET (or runoff), and 2) decompose decadal ET (or runoff) trends into the components that are caused by climate change and vegetation change. Zhang et al. (2001) were the first to couple water balance with vegetation dynamic using the Budyko model. Since then, dynamic information of vegetation type, rooting depth, and coverage was incorporated into the Budyko-type models in explaining the inter-annual and decadal variations in watershed water balance (Donohue et al., 2012; McVicar et al., 2007; Yang et al., 2009).

To demonstrate how vegetation may impact water balance, the dynamic of catchment water balance can be characterized as in Eq. (10) (Donohue et al., 2007). Water storage change (lefthand side of Eq. (10)), which is estimated as the complete differential of $Z{\cdot}S_w/\rho_w$, is balanced by the residue precipitation (P-ET-R). ρ_w is the density of water (kgm^{-3}), S_w is the density of water in the soil column (kgm^{-3}), Z is the vertical depth of the soil column, and A_c and τ are the spatial and temporal scales of analysis. The existence of vegetation affects catchment water balance by altering terms in Eq. (10). In theory, transpiration is a biophysical process that occurs through leaves driven by leaf photosynthesis. Vegetation affects ET by altering the transpiration and evaporation of intercepted water. Therefore, the most important vegetation parameter affecting ET is vegetation coverage (Donohue et al., 2007). Also, plants alter Z and S_w due to the variation of the rooting depth. A greater rooting depth usually implies that plants can draw water from a deeper layer of soil, and water storage changes of catchments were found to be correlated with rooting depth dynamics (O'Grady et al., 2011). Therefore, the rooting depth of plants can be a key indicator of vegetation impact on

water balance at inter-annual (Field et al., 1992) and intra-annual (Pate and Bell, 1999) time scales.

$$\frac{1}{\rho_w}\left(S_w\frac{\Delta Z}{\tau}+Z\frac{\Delta S_w}{\tau}\right)=\frac{P-ET-R}{\rho_w A_c} \tag{10}$$

Besides, it is usually assumed that ET is favored on forested catchments because forests intercept a higher proportion of rainfall and have higher soil water-holding capacities than other plants (Milly, 1994). For example, by reviewing 290 studies around the world, Canadell et al. (1996) showed that the maximum rooting depth of trees (7.0 ± 1.2 m) is generally greater than that of shrubs (5.1 ± 0.8 m) and herbaceous plants (2.6 ± 0.1 m). Such a difference in maximum rooting depths of trees and herbaceous plants can be translated to a 540 mm difference in plant-available water for sandy soils (Zhang et al., 2001). Therefore, vegetation type may be a crucial factor in the catchment water balance. In this section, we provide a detailed introduction to how the Budyko framework incorporates the dynamic information of vegetation type, coverage, and rooting depth to explain the interannual variations in watershed water balance.

3.1. The effects of land-cover type

The different impacts between forests and herbaceous plants come primarily through the plant-available water capacity. Therefore, Zhang et al. (2001) introduced an adjustable parameter w to discriminate the available water of forest catchments from herbaceous catchments, as shown in Eq. (11). The actual ET of a catchment can be modeled as the sum of respective contributions from the forest (f) and herbaceous vegetation (1-f), as shown in Eq. (12), where the best fit values of w were calibrated as 2.0 and 0.5 for forests and herbaceous plants, respectively, using global datasets (mainly from Australia, United States, and Africa).

$$\frac{ET}{P}=\frac{1+w\frac{ET_0}{P}}{1+w\frac{ET_0}{P}+\left(\frac{ET_0}{P}\right)^{-1}} \tag{11}$$

$$\frac{ET}{P}=f\frac{1+w_1\frac{ET_0}{P}}{1+w_1\frac{ET_0}{P}+\left(\frac{ET_0}{P}\right)^{-1}}+(1-f)\frac{1+w_2\frac{ET_0}{P}}{1+w_2\frac{ET_0}{P}+\left(\frac{ET_0}{P}\right)^{-1}} \tag{12}$$

Since the work of Zhang et al. (2001), the Budyko-type model that discriminates between forest and herbaceous vegetation was intensively used in assessing the effect of forest changes on water balance (McVicar et al., 2007; Sun et al., 2005; Sun et al., 2006; Van Dijk et al., 2007; Zhang et al., 2008b). A decision support tool for runoff impacts of forest changes can be developed using the above model (McVicar et al., 2007), where forest clear-cutting effects on water yield can be approximated by reducing the w parameter from w_1 (2.0) to w_2 (0.5) (Sun et al., 2005). For example, annual water yield increase would range from 440 mm/y in the wet region to less than 50 mm/y in the dry region, if the forest was removed in the southeastern United States (Sun et al., 2005). Streamflow will decrease by 9.2% if forest coverage increases from 8.1% to 18.2% in the middle of the Loess Plateau (Zhang et al., 2008b).

Following the work of Zhang et al. (2001), Oudin et al. (2008) conducted an international assessment on whether the land cover makes a significant contribution to the mean annual streamflow. They incorporated land-use information (Forest, cropland, grassland, heath, and non-vegetated land) into the equation of Zhang et al. (2001), and other four equations which are from Schreiber (1904), Ol'Dekop (1911), Turc (1954), and Budyko (1974). Annual runoff was modeled as the fraction-weighted sum of runoff from each land cover type (LC_i), as shown in Eq. (13), where Q_i is the mean annual streamflow for the part of the catchment covered by the ith land cover type. Q_i was computed using the modified formulations with an added parameter w_i. By comparing the original and the reformulated equations (with parameters calibrated) using data from 1508 catchments, Oudin et al. (2008) found that introducing extra degrees of freedom (parameters) into the 5 original formulas improves overall model performances; and land cover information contributes a small but significant to this improvement. By calibrating Zhang et al. (2001)'s equation using their global datasets, Oudin et al. (2008) found that the ET for arable land was the largest (w = 1.9), followed by forests (w = 1.2), and grassland (w = 0.7). ET for shrubland was the smallest (w = 0.1) (Fig. 2B).

$$Q=\sum_i LC_i\cdot Q_i \tag{13}$$

Worth noting, in contrast to the results of Zhang et al. (2001), Oudin et al. (2008) found that the best fit w value of forests (w = 1.2) is not significantly larger than the lumped value (w = 1.1) of the whole catchments. In addition, ET for forests was not the largest among all land cover types in Oudin et al. (2008)'s paper. Such results indicate that the plant-available coefficient needs local calibration. For example, Zhang et al. (2008b) used hierarchical cluster analysis to define 3 meta-groups in the space of ET/P and ET_0/P and regionalized the w values for herbaceous plants as 1.61, 0.45, and 0.10 along a climate dryness gradient in the Loess Plateau of China.

3.2. The effects of effective rooting depth

Roots of plants affect the partitioning of precipitation by altering the water storage capacity of the basin. Compared to the plant-available water coefficient, the rooting depth of plants is a more direct and physically-based parameter. Therefore, efforts have been paid to incorporate the rooting depth dynamics into the Budyko framework (Donohue et al., 2012; Porporato et al., 2004; Yang et al., 2016; Zhang et al., 2018b). Note that data of root profiles are scarce across the globe (Canadell et al., 1996; Schenk and Jackson, 2002), the effective (hydrologically active) rooting depth Z_r (m) concept is usually used as a surrogate of actual rooting depth. Z_r is defined as the total depth to which plant-accessible water can be stored (Donohue et al., 2012; Porporato et al., 2004), with typical values range from 0–2000 mm (Yang et al., 2016). Z_r is usually estimated using optimization approaches under the assumption that plants will act to minimize their water stress or to maximize productivity (Collins and Bras, 2007; Kleidon and Heimann, 1998; van Wijk and Bouten, 2001). Donohue et al. (2012) used the formulation of Guswa (2008) that balances the marginal carbon cost and benefit of deeper roots to estimate the spatial distribution of effective rooting depth (Description of Guswa's model is provided in the Appendix).

Z_r and the mean storm depth (α) exert opposite effects on runoff because large runoff may be produced by large storms (large α) or small retention capability (small Z_r) of the basin. Z_r/α is linearly related to the parameter n of the Choudhury-Yang model when the dryness index ET_0/P equals 1 (Donohue et al., 2012), i.e., $n = 0.21kZ_r/\alpha + 0.6$, where k is dependent on the soil texture. By linking n with Z_r and α, Donohue et al. (2012) therefore incorporated the effects of rooting depth and rainfall seasonality into the Choudhury model. They found that the incorporation of Z_r increased the accuracy in runoff prediction by 10% compared to the default simulation (n = 1.9) in wet catchments (runoff >500 mm/y) for the Murray-Darling basin, Australia. In addition, the runoff was found to be sensitive to Z_r, especially in the dry areas of the Murray-Darling Basin.

Note that the linear relationship between n and Z_r is only valid when the dryness index ET_0/P equals 1. At any P and ET_0 conditions, the $n \sim Z_r$ relationship can be numerically solved as in Eq. (14) and (15) (Yang et al., 2016), where θ is the plant-available water content which is determined by the soil property. By parameterizing Z_r model of Guswa (2008) at a global scale during 1982–2010, Yang et al. (2016) found that the incorporation of the $n \sim Z_r$ relationship produced satisfactory ET predictions at watershed scales compared to water-balance measurements in 32 major catchments across the globe (R^2 = 0.94, RMSE = 74 mm/y), and at grid-scale compared to the PML ET products (Zhang

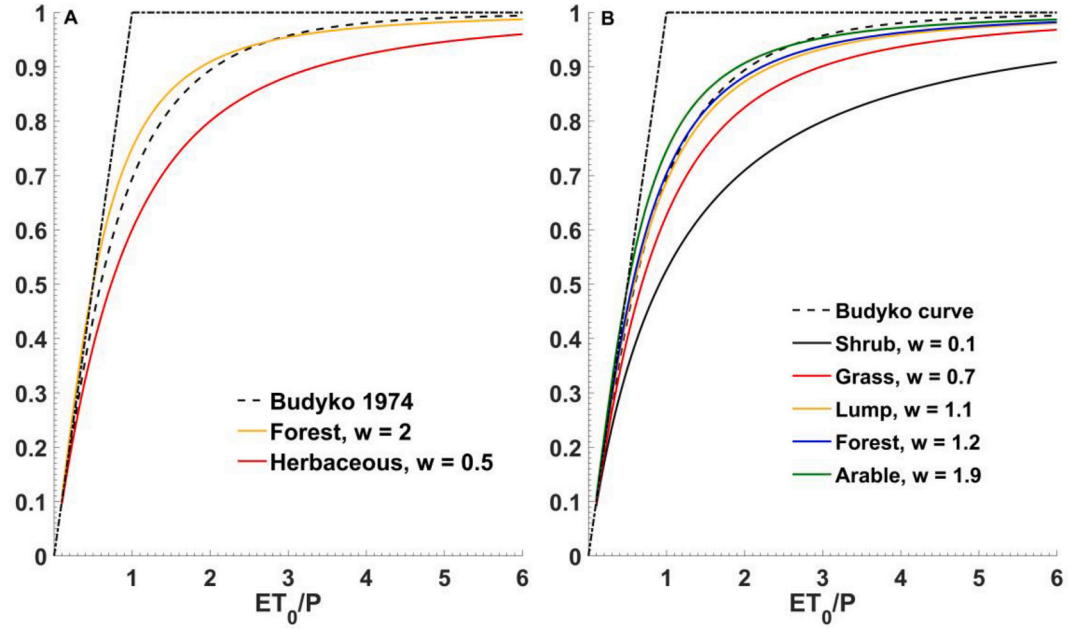

Fig. 2. Characterization of vegetation effects on annual water balances using Budyko curves with different values of plant-available water coefficient (w), (A) Forests and herbaceous plants were discriminated in Zhang et al. (2001), and (B) w were taken as 0.1, 0.7, 1.2, and 1.9 for shrubland, grassland, forests, and arable land, respectively, in Oudin et al. (2008).

et al., 2016b) ($R^2 = 0.90$, RMSE = 125 mm/y).

$$n = a log_{10}\left(\frac{Z_r\theta}{\alpha}\right)^2 + b log_{10}\left(\frac{Z_r\theta}{\alpha}\right) + c \tag{14}$$

$$\begin{cases} a = -0.003 log_{10}\left(\frac{ET_0}{P}\right)^2 + 0.247 log_{10}\left(\frac{ET_0}{P}\right) + 0.19 \\ b = -0.022\frac{ET_0}{P} + 0.403 \\ c = -0.071 log_{10}\left(\frac{ET_0}{P}\right)^2 - 0.332 log_{10}\left(\frac{ET_0}{P}\right) + 0.761 \end{cases} \tag{15}$$

The joint impacts of Z_r and α on water balance were shown in Fig. 3. Under a given rainfall seasonality condition, e.g., α = 20 mm (Fig. 3 B),

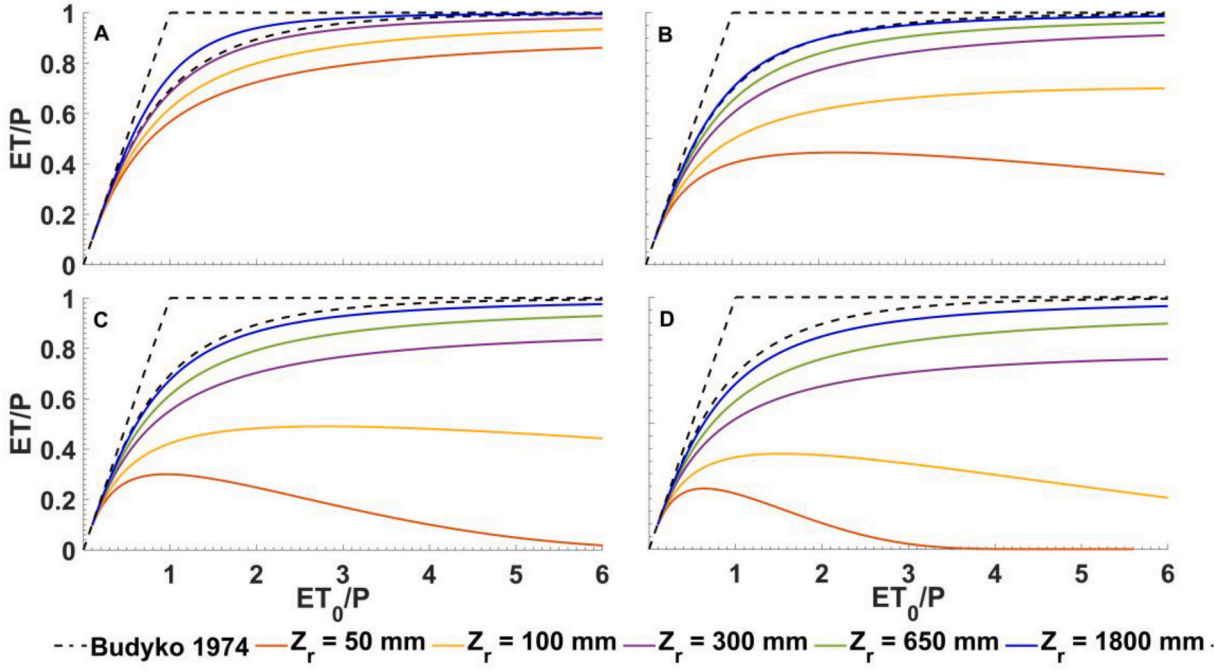

Fig. 3. Annual $ET_0/P \sim ET/P$ curves from the BCP model (Yang et al., 2016) under conditions with different values of Z_r (50, 100, 300, 650, 1800 mm) and α (5, 100, 300, 650, 1800 mm). (A) α = 5 mm; (B) α = 20 mm; (C) α = 35 mm; (D) α = 50 mm.

annual ET increases with Z_r significantly when Z_r was smaller than 300 mm, and ET predictions tend to converge to the Budyko curve when Z_r was larger than 650 mm (Fig. 3 B). Annual ET is higher than the Budyko curve predictions if the rainfall is more uniformly distributed e.g., $\alpha = 5$ mm (Fig. 3 A). Seasonality exerts significant impacts on annual ET, i.e., annual ET significantly decreases when α increases under the same dryness and rooting depth condition. Specifically, when rainfall events generally consist of large storms ($\alpha > 50$ mm, Fig. 3 D), $ET_0/P \sim ET/P$ curve no longer increases monotonically with the climate dryness index if the watershed retention ability is low (small Z_r, e.g., $Z_r = 50$ mm).

3.3. The effects of vegetation coverage

Vegetation coverage fraction (f_c) can now be readily obtained at watershed scales from the remotely sensed Normalized Difference Vegetation Index (NDVI) or leaf area index (LAI). Therefore, f_c is usually used to indicate vegetation's impact on water balance. For example, the spatial pattern of the parameter of Fu's equation (ω) is linearly correlated with the f_c spatial pattern in the large basins ($> 3.0 \times 10^5$ km^2) across the globe (Li et al., 2013). A simple regression equation $\omega = 2.36f_c + 1.16$ ($R^2 = 0.63$) was established based on the spatial correlation between ω and f_c using data from 26 large watersheds, including Amazon, Congo, Mississippi, Nile, and Yangtze river basins, etc. Reasonable annual ET predictions (RMSE = 47 mm/year) were yielded with the ω parameterization. In comparison, Fu's model produced worse results (RMSE = 76 mm/year) with the default value ω of 2.6. The linearity between the shape parameter and f_c over large watershed is due to that the vegetation cover itself reflects the overall influences of climate seasonality, soil parameters, topographic features, etc., at large scales (Li et al., 2013). In contrast, ω exhibited substantial variations around $2.36f_c + 1.16$ when Fu's model was applied to 232 smaller ($<1.0 \times 10^5$ km^2) catchments (Duan et al., 2006), indicating that f_c is coupled with other catchment properties at small watersheds, which are usually in non-steady-state and exhibit more heterogeneityin land surface properties.

For example, Yang et al. (2009) analyzed the influences of f_c on water balances in 99 non-humid small catchments in the Yellow River basin (Eq. 16), and the Huai River basin (Eq. 17) of China during the 1982–2000 period, where K_s/i_r and tanβ are the infiltration capacity and average slope of the catchment. At the global scale, NDVI is positively correlated with ω in small catchments (Xu et al., 2013). Together with latitude, topographic factor (CTI), catchment area, and elevation (*elev*), a regression equation (Eq. (18)) using NDVI explains 63% variances in ω for small watersheds. Note that vegetation properties (such as vegetation types and rooting depths) can be quite different under the same vegetation coverage condition, caution interpretations are needed when f_c is used with the Budyko framework at small scales.

$$n = 5.755\left(\frac{K_s}{i_r}\right)^{-0.368} f_c^{\,0.292} exp(-5.428 tan\beta) \tag{16}$$

$$n = 2.721\left(\frac{K_s}{i_r}\right)^{-0.3393} f_c^{\,-0.301} exp(4.351 tan\beta) \tag{17}$$

$$\omega = 5.05722\text{-}0.09322\text{lat} + 0.13085\text{CTI} + 1.31697\text{NDVI} + 0.0003\text{A}\text{-}0.00018\text{elev} \tag{18}$$

4. Vegetation effects on decadal water balance using the Budyko model

Shape parameters of Budyko-type models are capable of indicating vegetation dynamics, as shown in the last section. The incorporation of dynamic information of vegetation type, coverage, and effective rooting depth has also proved to be crucial in explaining the interannual variations in catchment ET and runoff. For example, Liu et al. (2018)'s analysis on large basins ($> 3.0 \times 10^5$ km^2) across the globe revealed that vegetation dynamics remarkably impacted the temporal variation in n, explaining 67% of the variance.

Besides interannual variations, vegetation may experience greening or browning trends at a decadal scale. For example, vegetation greening has occurred globally during the last several decades (Chen et al., 2019; Zhu et al., 2016). At a decadal scale, the multi-year average of runoff during the pre-change period (e.g., 1960–1980) may be quite different from the post-change period (e.g., 1981–2000) due to the vegetation change. However, because the climate is also changing at a decadal time scale, quantifying the relative contribution of vegetation change and climate change to the water balance changes has become an important aspect for developing sustainable water resources plans (Zhang et al., 2018a).

To solve this problem, the difference in catchment runoff (ΔR) between two periods can be viewed as the sum of the impacts by climate change (ΔR_C) and land-use change (ΔR_H), as shown in Eq. (19). Because the Budyko models established the relationship between R and climate conditions explicitly, the sensitivity of R (or ET) with respective to P and ET_0 can be readily derived. ΔR_C can then be determined by the elasticity method (Dooge et al., 1999; Koster and Suarez, 1999; Sankarasubramanian et al., 2001), which estimated ΔR_C by multiplying the sensitivity coefficients of P and ET_0 (f'_P and f'_{ET0}) with the respective changes in P and ET_0 (ΔP and ΔET_0), as shown in Eq. (20).

$$\Delta R = \Delta R_C + \Delta R_H \tag{19}$$

$$\Delta R_C = f'_P \Delta P + f'_{ET_0} \Delta ET_0 \tag{20}$$

The sensitivity coefficients of R with respect to P and ET_0 are shown in Eq. 21 using Fu's model (Ma et al., 2008). Combining the elasticity method with Fu's model, Wang and Hejazi (2011) reported that climate change induced an 18% increase in R during the 1971–2003 period in the contiguous United States compared to the 1948–1970 period. Therefore, human impacts ($\Delta R_H = \Delta R - \Delta R_C$) induced a 16% (absolute) change in R. Further analysis found that the most correlated factor with ΔR_H was cropland percentage ($R^2 = 0.86$), indicating that vegetation change will exert the most critical impact among all human activities in catchment runoff.

$$f'_P = P^{(\omega-1)}\left(ET_0^{\omega} + P^{\omega}\right)^{(1/\omega-1)} \tag{21a}$$

$$f'_{ET_0} = ET_0{}^{(\omega-1)}\left(ET_0^{\omega} + P^{\omega}\right)^{(1/\omega-1)} \tag{21b}$$

Similarly, the impacts of land-use change can be characterized analytically using the sensitivity expression of shape parameters. For example, based on the Choudhury-Yang model, sensitivity coefficients of ET to P, ET_0, and n were expressed as eq. 22 (Roderick and Farquhar, 2011). Therefore, the relative change in runoff (ΔR/R) is expressed as the sum of the changes that are induced by P, ET_0, and n (Eq. (23)) under the steady-state assumption. Relative contribution by vegetation change can then be further apportioned by incorporating the parameterizations of model parameters (ω and n, Section 3).

$$\frac{\partial ET}{\partial P} = \frac{ET}{P}\left(\frac{ET_0^n}{ET_0^n + P^n}\right) \tag{22a}$$

$$\frac{\partial ET}{\partial ET_0} = \frac{ET}{ET_0}\left(\frac{P^n}{ET_0^n + P^n}\right) \tag{22b}$$

$$\frac{\partial ET}{\partial n} = \frac{ET}{n}\left(\frac{ln\left(ET_0^n + P^n\right)}{n} - \frac{ET_0^n ln ET_0 + P^n ln P}{ET_0^n + P^n}\right) \tag{22c}$$

$$\frac{\Delta R}{R} = \left[\frac{P}{R}\left(1 - \frac{\partial ET}{\partial P}\right)\right]\frac{\Delta P}{P} - \left[\frac{ET_0}{R}\frac{\partial ET}{\partial ET_0}\right]\frac{\Delta ET_0}{ET_0} - \left[\frac{n}{R}\frac{\partial ET}{\partial n}\right]\frac{\Delta n}{n} \tag{23}$$

Due to its robustness and transparency, the Budyko-type models were intensively used to study the joint impacts of climate and vegetation on water balances (Zhang et al., 2018a), for example, at a regional scale (Ahn and Merwade, 2014; Jiang et al., 2015; Wiekenkamp et al., 2016; Xu et al., 2014; Ye et al., 2013), continental-scale (Abatzoglou and

Ficklin, 2017; Smettem and Callow, 2014; Voepel et al., 2011; Ye et al., 2015), and global scale (Liu et al., 2018; Wei et al., 2018; Zhou et al., 2015). For example, at the global scale, Wei et al. (2018) assessed relative contributions of vegetation and climate change to annual runoff variations from 2000 to 2011 in forested watersheds (forest coverage >30%) using the Fu model and the Choudhury-Yang model and found that change in vegetation cover contributed up to 30.7% ± 22.5% of the changes in annual runoff across the globe.

Significant impacts of vegetation in water balance changes were intensively reported at regional and continental scales (Jaramillo et al., 2018; Liu et al., 2017; Liu et al., 2019; Shen et al., 2017). For example, the movements in Budyko space could not be explained by climatic changes in 60% of the catchments in Sweden, where forest biomass has increased during the last 6 decades; instead, standing forest biomass was the most significant factor that could explain most of the variance (Jaramillo et al., 2018). In southwestern Australia, P, ET_0 and ω contributed 45.4%, 7.2%, and 47.4% to the decline in the annual runoff during two periods of 1970–2000 and 2001–2015 (Liu et al., 2019). Further analysis revealed that NDVI was the only significant factor that controlled the variation in ω. In addition, Liu et al. (2017)'s analysis revealed that changes in climate and underlying surface contributed almost equally (53.5% v.s. 46.5%) to the runoff changes in major catchments of China. Human impacts were dominant factors in runoff changes in some catchments of northeastern and northern China (Shen et al., 2017), especially in Loess Plateau, where ecological restoration contributed more than climate change (62% v.s. 38%) for the runoff decline (Liang et al., 2015). As stated by Roderick and Farquhar (2011), vegetation change is the dominant factor in changes of the underlying surface because the vegetation can readily change over decades, whereas geologic and topographic properties of a given catchment remain nearly constant over decadal to century time scales. Therefore, the significant contribution of ω and n, usually indicate large impacts of vegetation on water balances.

5. Dependence of vegetation role on climate

Recent studies have shown that the Budyko framework can be extended to provide insights into the interdisciplinary topics that concern climate, hydrology, and ecology (Donohue et al., 2012; Gentine et al., 2012; Troch et al., 2013). The incorporation of dynamic processes of vegetation (e.g., rooting depth variation) has proved valuable in explaining interannual and decadal variations of catchment water balance. However, although relative contributions of climate change and vegetation change to the decadal water balance changes have been intensively studied in recent years, vegetation and climate are not independent factors affecting water balance. Ultimately, the growth of vegetation is strongly dependent on climate (Yang et al., 2009). To gain deeper insights into the understanding of climate-water-vegetation interactions using the perspectives from Budyko framework, we discuss the following eco-hydrological issues that pertain to the Budyko model in this section: 1) how does vegetation effect differ under different climate conditions and 2) how the coupling between vegetation and climate seasonality at an intra-annual scale affects catchment water balance at an interannual scale.

5.1. Different vegetation response across different climate conditions

It has been long recognized that under water stress, vegetation canopy tends to adjust stomatal conductance to improve water use efficiency at leaf scale (Farquhar and Sharkey, 1982; Hall and Schulze, 1980), or adjust root growth to maximize carbon assimilation (Guswa, 2008) and maintain transpiration at plot scale. However, the responses of vegetation to water shortage are different under different water and energy conditions. Measurements of root profiles showed that the rooting depths of plants are generally positively correlated with energy supply (ET_0) across the globe, however, rooting depths of temperate and boreal forests increases with precipitation, whereas rooting depths of grassland, shrubland, and savannas are negatively correlated with precipitation (Schenk and Jackson, 2002). At the catchment scale, the difference in annual ET between forested catchment and non-forested catchment was found to be larger in areas with higher rainfall and diminishes in areas with annual rainfall less than 500 mm (Zhang et al., 2001). Such a result at the catchment scale is consistent with the plot-scale root profile measurements because as precipitation increase, the rooting depth of forest tend to increase whereas that of non-forest tend to decrease, ET of the forested areas is therefore possibly larger than that of non-forested areas.

Also, the notion that vegetation responses differ across climate conditions helps to interpret different opinions in the relative contribution of vegetation types in different Budyko-model related works. For example, Zhang et al. (2001) concluded that ET from forest catchments is higher than from non-forest catchments, whereas Oudin et al. (2008) arrived at contrary conclusions that the best fit w value of forests (w = 1.2) is not significantly larger than the lumped value (w = 1.1) of the whole catchments and ET for forests was not the largest among all land cover types. Such contrasts were due to at least two reasons. Firstly, different approaches (PT and PM) were used in estimating ET_0 in these two papers. Different ET_0 values may result in different w values. Secondly and more importantly, climate conditions of catchments were much dryer in Zhang et al. (2001) than those in Oudin et al. (2008). Water is the limiting factor ($ET_0/P > 1$) for ET in most of the catchments in Zhang et al. (2001), whereas water supply is not the limiting factor ($ET_0/P < 1$) in most of the catchments in Oudin et al. (2008). Therefore, a higher w (2.0 *v.s.* 1.2) value for forests was resulted in Zhang et al. (2001)'s work, indicating that the difference between forest ET and herbaceous ET may be more significant in conditions with larger aridity index. In contrast, when water is not a limiting factor, ET from the forest is not significantly larger than that from other plants (Oudin et al., 2008).

Water supply conditions alter vegetation's impacts on water balances. For example, forests growing under dry conditions showed higher hydrological resilience to drought compared to those growing under more humid conditions (Helman et al., 2017). Similarly, the w values for herbaceous plants were found to decrease with climate dryness in a quadratic way (Zhang et al., 2008b), indicating that the effect of forests is more significant in dryer conditions. Zhang et al. (2016a)'s analysis on 52 catchments ($0.08–3.8 \times 10^4$ km^2) in northern China showed that the sensitivity of n to f_{PAR} is not constant, instead, n is more sensitive to f_{PAR} at higher dryness conditions, i.e., $\Delta n/\Delta f_{PAR} = 0.02(ET_0/P)^{2.6}$, where f_{PAR} is the fraction of Photosynthetically Active Radiation absorbed by vegetation. Such results indicated that the shape parameters of Budyko models are not independent of climate conditions.

$ET_0/P = 1$ proves to be a critical value in understanding climate-water-vegetation interactions. The runoff coefficient (R/P) is more responsive to catchment properties when $ET_0/P > 1$ (non-humid) than it is when $ET_0/P < 1$ at the global scale (Zhou et al., 2015), suggesting that vegetation changes will lead to greater hydrological responses in non-humid conditions than in humid conditions. Note that rooting depth increases with ET_0/P and peaks in sub-humid environments ($ET_0/P \approx 1$) (Schenk and Jackson, 2002), and Z_r is generally larger in wetter conditions than in water-limited conditions (Fig. 3 in Guswa (2008)). Due to deeper roots, such an analysis helps to explain the result that R/P is more robust in wetter conditions. In summary, we want to note here that the different vegetation roles under dry/wet conditions need to be accounted for in Budyko applications and interpretations.

5.2. Coupling of vegetation with climate seasonality

Seasonality of rainfall, e.g., the mean storm depth and the frequency of rainfall, have been incorporated analytically into the Budyko-type models using stochastic approaches (Milly, 1993; Porporato et al., 2004), as shown in Eqs. (8) and (9). In addition, joint control of effective

rooting depth and mean storm depth on annual water balance was also explored (Fig. 3). Phase difference usually exists between P and R_n, which is a crucial factor for the vegetation characteristics. However, the phase difference at the intra-annual scale was not considered in their studies (Milly, 1993; Porporato et al., 2004).

In water-limited regions such as the Loess Plateau of China, the phase difference between P and ET_0 can account for 0.1% ~ 74.8% of the ET variations (Ning et al., 2017). ET would be larger if P and ET_0 are in-phase throughout the year. Large phase difference favors small ET and large vegetation fraction favors large ET, as shown in Eq. (24) (Ning et al., 2017), where the seasonality index (SI) is defined using the ratios of the amplitudes of the monthly harmonics to the monthly averages of P and ET_0 (δP and δET_0, Eq. (25)) (Woods, 2003) to represent the non-uniformity in the intra-annual distribution of water and energy. The seasonal fluctuation of the difference between P and ET_0 would be zero if $SI = 0$. Joint control of phase-difference and vegetation exists not only in water-limited regions but also broadly across the globe, and phase-difference alone can account for over 50% of the variances in the parameter n at the global scale (Liu et al., 2018).

$$\omega = 1 + 3.683 f_c^{0.798} \cdot exp(-0.246 SI) \tag{24}$$

$$SI = \left| \delta P - \delta ET_0 \cdot \frac{\overline{ET_0}}{\overline{P}} \right| \tag{25}$$

Phase-difference is a crucial factor for water balance, which is partly due to its impacts on vegetation characteristics. Schenk and Jackson (2002) compiled 475 root profiles from 209 locations around the world, and they found that plants in a climate with an obvious phase lag between energy and water availability (e.g., Mediterranean climate) tend to preserve a deeper rooting structure to cope with water stress. Gentine et al. (2012)'s analysis on the MOPEX data (Duan et al., 2006) revealed that rooting depth increases with τ_P - τ_{ET0} when τ_P - τ_{ET0} is larger than 1 month, where τ_P and τ_{ET0} are the time when P and ET_0 approach their maximum throughout the year. Rooting depth reaches its minimum when τ_P - τ_{ET0} is negative. In contrast, without plant adaptation, annual ET would be smaller if precipitation and radiation are out-of-phase (Feng et al., 2012). It is worth noting that the phase difference between P and ET_0 needs to be explicitly incorporated when Budyko models are used in vegetation applications.

6. Limitations and possible solutions

6.1. Trade-offs between parameters

Although numerous parameterizations on shape parameter of Budyko models have been established, tradeoffs may exist among explanatory factors, for example, regression analysis found that f_c and watershed slope exerted positive and negative impacts on parameter n, respectively, in two watersheds in China (Eq. (16) and (17)) (Yang et al., 2009). Similarly, contrary to the study at large scale across the globe, Bai et al. (2019)'s analysis showed that ω is negatively correlated with the remotely sensed vegetation greenness index for catchments that are smaller than 10^5 km^2 in China. They attributed such a negative correlation to the spatial scale. However, it is uncertain whether such results are due to different climatic/scale conditions, or merely tradeoffs among factors caused by regression.

In most of the previous studies, only runoff data (or P - R) were used to parameterize Budyko-type models. Therefore, tradeoffs may exist among explanatory factors if the calibration is performed against a single target. Fortunately, nowadays, ET can be obtained using the eddy covariance technique (Aubinet et al., 2000) with reasonable accuracy at 10^2–10^3 m scales (Baldocchi et al., 2001; Haughton et al., 2018) and regional scales by remote sensing retrievals (Kustas et al., 1999; Mu et al., 2011). Such progress may serve as a great help in Budyko applications. For example, to assess the inter-annual and intra-annual variability in water balance at subbasins of the Heihe watershed of China, which are unclosed watersheds with significant root zone water storage changes and inflow from the upper sub-watersheds, Du et al. (2016) parameterized and validated a two-parameter Budyko-type model using both of the monthly runoff data and ET data from remote sensing retrievals. Based on the remote sensing ET data from the University of Montana (UM) and monthly runoff data, Chen et al. (2013) extended the usage of a Budyko-type model to discriminate the wet-season and dry-season ET. Similarly, Cheng et al. (2011) found a linear interannual relationship between ET/P and ET_0/P across the contiguous United States by analyzing the UM-ET data, and they partly attributed such linearity to the adaptation of vegetation to the interannual variability of climate.

To disentangle the contribution of vegetation from other catchment properties, Gerrits et al. (2009) modeled interception evaporation and plant transpiration separately as a stochastic process at daily and monthly time scales and then up-scaled the results to annual scales based on the rainfall distribution function. Note that ET measurements can be further partitioned into its biological and abiological components based on isotope technique (Gibson and Edwards, 2002), sap flow technique (Liu et al., 2015), water-carbon correlation characteristics (Scanlon and Sahu, 2008; Zhou et al., 2016; Gan and Liu, 2020) and model simulations (Gan and Gao, 2015; Gao et al., 2016b). With the development of remote sensing, upscaling of ET components from local to regional scales has also been intensively studied (Gan et al., 2019; Song et al., 2018). For example, Nijzink et al. (2016) used the estimate of transpiration to reproduce the temporal evolution of root-zone storage capacity under change. To better resolve vegetation dynamics within the water-energy balance framework, we suggest that more detailed datasets are used besides runoff observations, including the transpiration of different vegetation, evaporation from vegetated and non-vegetated areas, etc.

6.2. Overlook of water storage

It is noteworthy that when the Budyko models are applied at a long-term scale ($>>1$ year), the variations of water storage in the basin can be neglected ($\Delta S = 0$) (Gerrits et al., 2009; Milly, 1993; Porporato et al., 2004). ΔS is defined as the difference of terrestrial water storage between the current and the previous time point, which equals to the residue precipitation (P – ET – R). When Budyko-type models are applied at the annual and intra-annual scales, the ignorance of ΔS may produce huge errors (Wang et al., 2009; Wang et al., 2018; Zeng and Cai, 2015; Zeng and Cai, 2016). For example, the annual storage change ratios (ΔS/P) were found to vary from −60% to 40% at the watersheds in Illinois, US (Wang, 2012). In dry years, ΔS can even be as twice as the annual runoff in the southeast Australia (Leblanc et al., 2009). Therefore, an evident shift of annual water balance in the Budyko space was observed for the catchments with significant groundwater-dependent ET, e.g., in Australia and Northern-central China (O'Grady et al., 2011; Wang and Zhou, 2016). Soil water and groundwater sustain the baseflow and ET between the interval of two precipitation events. Without considering the ΔS term, (P - R)/P can even be negatively correlated with the aridity index, which violates the Budyko hypothesis, e.g., in the Sand Hills region of Nebraska, USA (Wang et al., 2009). Zeng and Cai (2016) also found that the inter-annual variability in ET is mainly controlled by ΔS in the Middle Asian regions.

Wang (2012) found that the inter-annual variations in ET were correlated with P-ΔS instead of P at 12 watersheds in Illinois, USA, by analyzing the long-term records of soil moisture and groundwater level data. To take the influence of ΔS into account, Wang (2012) defined a concept of effective precipitation as the difference between precipitation and water storage changes (P-ΔS), and replaced the precipitation by effective precipitation in the Budyko equation at an annual scale. With the development of remote sensing technique, the remotely sensed ΔS, such as that using the GRACE satellite data (Jiang et al., 2014; Long et al., 2015) have played an important role in the application of water-

energy balance models (Fang et al., 2016; Tang et al., 2017). The incorporation of hydrological signatures that are derived from the GRACE signal, including the GRACE amplitude, interannual variability, and 1-month lag autocorrelation, was found to reduce the simulation errors by 50% when the Budyko-type equations were applied at the US basins (Fang et al., 2016). Recently, Xing et al. (2018b) downscaled the GRACE ΔS data from 1° to 0.25° based on the land surface model simulations (Wan et al., 2015), and applied the water-energy balance equation with the downscaled ΔS data to 24 watersheds in different climatic regions of China. The estimated monthly average ET accuracy exceeded the accuracy of the land surface process model.

We want to note here that the overlook of water storage will not only introduce errors in ET estimation but also hinder the analysis of vegetation effect on water balance. When resolving vegetation dynamics within the Budyko framework, the control of ΔS on transpiration and soil evaporation should be explicitly considered. However, although the GRACE data have been widely used to assess water storage changes in hydrological applications and several papers have applied the Budyko-type with the GRACE data (Fang et al., 2016; Tang et al., 2017; Xing et al., 2018b), due to its coarse spatial resolution, the GRACE data are better suited to relatively large basins ($> \sim 10^5$ km^2). In addition, Gnann et al. (2019) conducted a study on whether there exists a "Budyko curve" for the baseflow and found that the aridity index is not always a good indicator of baseflow fraction, indicating that the partitioning of ΔS into runoff and ET may be different to that of precipitation. Moreover, under wet and dry conditions, the ET/ΔS ratios differ from each other substantially (Chen et al., 2013), which makes groundwater-vegetation interactions more complicated.

6.3. Lacks of vegetation-coevolution representation

Vegetation dynamic information is not incorporated in the original derivation of Budyko models, although a key aspect delivered in Budyko (1974) is the coevolution of climate and life. The uncertainty of the original Budyko curve at long-term scales is within 10% (Gentine et al., 2012), which is reasonable compared to the observational errors in precipitation and streamflow measurements (Potter et al., 2005). This leads to an interesting question that why vegetation effect may be minimal at long-term scales and how all factors (climate, soil texture, and vegetation, etc.) interact to produce such a simple curve? Troch et al. (2013) speculated that vegetation's coevolution with climate may explain such a contradiction. Transpiration efficiency and rooting structure of the plants are found to be adaptable to the dryness index and the phase lag between peak radiation and precipitation (Gentine et al., 2012), indicating that any climatological change may result in a corresponding vegetation adaptation to bring the water balance of a catchment back to the Budyko curve (van der Velde et al., 2014; Wang et al., 2016). For example, simulations in 12 US catchments with 12 different climate forcing indicated that anti-correlation existed between the effects of catchment characteristics and climate properties, i.e., catchments that developed in a climate that favors high E/P will produce low E/P on average in the 12 simulations (Troch et al., 2013). Under the vegetation-coevolution assumption, parameters of a model will be constrained in a way that the long-term ET predictions of the model are close to the climate-dependent estimates from, e.g., the original Budyko curve (Gentine et al., 2012). For example, Zhang et al. (2010) successfully used the long-term Budyko curve (Budyko, 1974) to calibrate the the parameters of a biophysical ET model across the Australian continent.

Because catchment properties (parameters) will adapt to the changing climate, the usage of hydrological models that are calibrated using historical data may produce bias in future predictions under climate change conditions (Milly et al., 2008; Sivapalan, 2006), especially under drier climate (Saft et al., 2015). For example, Saft et al. (2016) demonstrated that runoff was consistently overestimated due to climate-induced shifts in the rainfall-runoff relationship under prolonged dry conditions. Such a result indicates that results from the elasticity method (Dooge et al., 1999; Koster and Suarez, 1999; Sankarasubramanian et al., 2001) (Section 4) may be just first-order approximations to the decadal decomposition of relative contributions of vegetation and climate to the water-balance changes because the elasticity method assumes that vegetation and climate are independent factors. We want to note here that caution interpretations are needed when using the Budyko framework to identify the vegetation effects on water balance at a decadal scale because vegetation coevolves with the climate at this time scale. Moreover, climate stationarity is no longer a valid assumption under the climate change background (Milly et al., 2008).

Although a detailed theory of vegetation-coevolution has not been established, statistical approaches have been widely used to account for the climate-dependent vegetation effect. For example, Ning et al. (2017) established the joint control of vegetation and climate seasonality on the shape parameter n, and Zhang et al. (2016a) examined the climate dependence of the sensitivity of n to vegetation index. In addition, the "Darwinian approach" of catchment classification and space-time substitution strategy, as well as the optimality theory will be useful for addressing the vegetation coevolution issues with the Budyko framework.

Compared to the Newtonian approaches that concern with the mechanistic description of every individual piece of a system, the Darwinian approach explains the hydrologic behavior of hydrologic systems as a whole and studies the classification and evolution of the population of watersheds (Harman and Troch, 2014). By synthesizing pieces of evidence and explanations of the interactions between hydrological cycles and landscape features, Troch et al. (2015) proposed a conceptual framework to understand the catchment-coevolution process and suggested three independent drivers for the evolution of land surface features: tectonic uplift, geology weathering, and climate forcing. They stated that watersheds can be characterized and classified according to its "hydrologic age" (A), which is defined as follow.

$$ER = \frac{dA}{dt} = f(T(t), G(t), C(t)) \tag{26}$$

where ER is the evolution rate or rate of aging, T(t), G(t), and C(t) stand for the impacts of tectonic uplift, geology weathering, and climate forcing, respectively. Due to the long time scale of the catchment coevolution process, it is difficult (or even impossible) to collect a complete dataset of land features and hydrological responses for a specific watershed throughout its lifecycle, from its formation to the present stage. Therefore, the space-time substitution strategy is usually used in the catchment coevolution researches. The validity of the space-time substitution strategy lies in that similar phenomena at different locations follow similar evolutionary trajectories although the starting times of the phenomena are different (Harman and Troch, 2014). For example, Carmona et al. (2014) analyzed the regional patterns of interannual variability of catchment water balances across the Unite State using the Budyko framework and confirmed the existence of space-time symmetry between spatial variability and general trends in the temporal variability. They further classified the catchments into eight similar groups based on the magnitude of the ω parameter. Another example can be seen in Li et al. (2013), where the improved annual predictions of a watershed come primarily from the spatial ω-NDVI relationship of other watersheds.

It has long been assumed that water use efficiency (Caylor et al., 2009; Creed et al., 2014; Troch et al., 2013; Troch et al., 2009) and carbon gain profit (del Jesus et al., 2012; Raupach, 2005; Schymanski et al., 2010; Schymanski et al., 2009) may be the controlling factors of the direction of vegetation coevolution. The effective rooting depth Z_r is usually estimated using optimization approaches under the assumption that plants will act to minimize their water stress or to maximize productivity (Collins and Bras, 2007; Kleidon and Heimann, 1998; van Wijk

and Bouten, 2001). The incorporation of Z_r has been proved to be useful for the Budyko applications (Donohue et al., 2012; Yang et al., 2016). At a watershed scale, de Boer-Euser et al. (2016) estimated the influence of soil and climate on root zone storage capacity using the optimality theory.

Eagleson (1978a) and Eagleson (1982) developed a theoretical framework for climate-vegetation interactions based on the assumption that vegetation can act to minimize water stress. Such a framework has been used at a regional scale (Ellis et al., 2005). Similarly, Troch et al. (2009) hypothesized that vegetation tends to utilize the available soil moisture to the greatest extent. del Jesus et al. (2012) successfully reproduced the spatial organization of vegetation coverage by optimizing carbon assimilation in river basins. From the ecological perspective, vegetation is a key indicator in the eco-hydrological equilibrium state (Eagleson, 1978a; Eagleson, 1978b; Eagleson, 1982; Nemani and Running, 1989) of a catchment. Vegetation properties (e.g., LAI, or vegetation cover) can be used to indicate how far the catchment water balance deviates from its eco-hydrological equilibrium state. For example, results from the optimality frameworks that maximize LAI under given water available regimes were found to converge to predictions from the Budyko framework (O'Grady et al., 2011). Li et al. (2014) demonstrated how the Budyko curve emerges by running a simple distributed hydrologic model to simulate the effects of different combinations of climate, soil, and topography events. Similarly, optimal models that predict vegetation properties may be useful in explaining the emergence of the long-term Budyko curve by running the model under different climate, soil, and topography conditions.

7. Summary and concluding thoughts

Global vegetation has experienced great changes in recent decades, therefore, their effect on catchment water balance has been a hot topic in hydrology and global change studies. The Budyko models, which provide a transparent framework for analyzing the climate-water interaction, were intensively used to analyze how vegetation influences the partition of catchment precipitation into evapotranspiration and runoff. In this paper, we gave a thorough review of Budyko models' perspectives on the relation between vegetation dynamic and catchment ET (or runoff). By reviewing global and regional cases that studied the vegetation role using the Budyko models, we found that the variations in the shape parameters of Budyko curves are capable of indicating vegetation effects on catchment water balanceand the incorporation of effective rooting depth made the Budyko model explain over 90% of spatial variation in ET across the globe. In general, climate dominates the catchment water balance, however, forest changes also account for 30.7% ± 22.5% in annual runoff changes in forested watersheds across the globe. Vegetation effects differ across different climatic conditions, and the sensitivity of the shape parameter concerning vegetation indices increases non-linearly with climate dryness (ET_0/P). Vegetation effects differ across different climate seasonality conditions. Coupling between climate seasonality (rainfall frequency and the time lag between maximum precipitation and net radiation) and vegetation at the intra-annual scale is the most crucial factor in explaining variations in catchment water balance at annual scales.

As an emergent hydrological model that was derived from the hydrological responses from a variety of hydrological systems, the original Budyko curve represents the universal control of climate on the water partitioning of a watershed. Although vegetation dynamic information can be (statistically) incorporated into the Budyko framework at an annual scale, major knowledge gaps still exist, including 1) how the climate and land surface properties interact to produce such a simple curve that bears space-time symmetry? and 2) How to represent the vegetation-coevolution properties when the Budyko models are used in non-steady states? Future studies are needed to comprehensively incorporate climate seasonality and vegetation dynamic in an analytical way, e.g., by solving stochastic differentiate equations on soil moisture balance to explicitly demonstrate how seasonality-vegetation coupling at intra-annual scales affect water balance at an annual scale. In addition, vegetation-climate interaction properties, including how vegetation optimizes and coevolves with the climate at different climate conditions should be explicitly incorporated in future model derivation. To achieve this goal, detailed hydrological datasets are also needed to resolve the vegetation effect at fine spatial and temporal scales.

Declaration of Competing Interest

The authors declare that they have no known competing financial interests or personal relationships that could have appeared to influence the work reported in this paper.

Acknowledgements

Our research is jointly funded by the National Natural Science Foundation of China (42071054), the National Natural Science Foundation of China (41601033), the National Natural Science Foundation of China (51879255), and the Open Fund of State Key Laboratory of Remote Sensing Science (OFSLRSS202020).

Appendix A. Guswa's effective rooting depth model

Guswa (2008) obtained an analytical expression of the effective rooting depth by equating the marginal carbon cost and benefit of deeper roots. The average carbon cost ($C(Z_r)$, Eq. (A1)) of plant roots per unit area of ground surface is the function of the rate of root respiration (γ_r, mmol C/g/d), the specific root length (SRL, cm/g), and the root-length density (RLD, cm root/cm^3 soil). Similarly, the average carbon gain ($B(Z_r)$, Eq. (26)) of all roots per unit area is estimated by the transpiration rate (T), the water use efficiency (WUE) and the length of the growing season (f_{seas}). By forcing soil moisture dynamic by stochastic rainfall, an analytical expression is solved as a function of climate and soil characteristics (Eq. (A2)), where θ is available water for plant, w_T is the ratio of the mean rainfall rate to the mean rate of potential T, X is a function of α, θ, w_T and plant characteristics including γ_r, RLD, SRL, WUE and f_{seas}. Guswa (2008)'s model has been incorporated into the Budyko framework (Donohue et al., 2012; Yang et al., 2016; Zhang et al., 2018b).

$$C(Z_r) = \int_0^{Z_r} \frac{\gamma_r RLD}{SRL} dz \tag{A1}$$

$$B(Z_r) = WUE \cdot f_{seas} \cdot \langle T \rangle$$

$$Z_r = \frac{\alpha}{\theta(1 - w_T)} ln(X) \tag{A2}$$

References

Abatzoglou, J.T., Ficklin, D.L., 2017. Climatic and physiographic controls of spatial variability in surface water balance over the contiguous United States using the Budyko relationship. Water Resour. Res. 53 (9), 7630–7643.

Ahn, K.H., Merwade, V., 2014. Quantifying the relative impact of climate and human activities on streamflow. J. Hydrol. 515, 257–266.

Andreassian, V., Perrin, C., 2012. On the ambiguous interpretation of the Turc-Budyko nondimensional graph. Water Resour. Res. 48.

Arnell, N.W., Gosling, S.N., 2013. The impacts of climate change on river flow regimes at the global scale. J. Hydrol. 486, 351–364.

Arora, V., 2002. Modeling vegetation as a dynamic component in soil-vegetation-atmosphere transfer schemes and hydrological models. Rev. Geophys. 40 (2).

Aubinet, M., et al., 2000. Estimates of the annual net carbon and water exchange of forests: the EUROFLUX methodology. Adv. Ecol. Res. 30, 113–175.

Bai, P., Liu, X., Zhang, D., Liu, C., 2019. Estimation of the Budyko model parameter for small basins in China. Hydrol. Process. 0 (0).

Baldocchi, D., et al., 2001. FLUXNET: a new tool to study the temporal and spatial variability of ecosystem-scale carbon dioxide, water vapor, and energy flux densities. B Am. Meteorol. Soc. 82 (11), 2415–2434.

Beck, H.E., et al., 2013. The impact of forest regeneration on streamflow in 12 mesoscale humid tropical catchments. Hydrol. Earth Syst. Sc 17 (7), 2613–2635.

Bi, H.X., et al., 2009. Effects of precipitation and landuse on runoff during the past 50 years in a typical watershed in the Loess Plateau, China. Int. J. Sediment Res. 24 (3), 352–364.

Brown, A.E., Zhang, L., McMahon, T.A., Western, A.W., Vertessy, R.A., 2005. A review of paired catchment studies for determining changes in water yield resulting from alterations in vegetation. J. Hydrol. 310 (1–4), 28–61.

Budyko, M., 1974. Climate and Life. Academic, New York.

Canadell, J., et al., 1996. Maximum rooting depth of vegetation types at the global scale. Oecologia 108 (4), 583–595.

Carmona, A.M., Sivapalan, M., Yaeger, M.A., Poveda, G., 2014. Regional patterns of interannual variability of catchment water balances across the continental US: a Budyko framework. Water Resour. Res. 50 (12), 9177–9193.

Caylor, K.K., Scanlon, T.M., Rodriguez-Iturbe, I., 2009. Ecohydrological optimization of pattern and processes in water-limited ecosystems: a trade-off-based hypothesis. Water Resour. Res. 45.

Chen, X., Alimohammadi, N., Wang, D.B., 2013. Modeling interannual variability of seasonal evaporation and storage change based on the extended Budyko framework. Water Resour. Res. 49 (9), 6067–6078.

Chen, C., et al., 2019. China and India lead in greening of the world through land-use management. Nat. Sustain. 2 (2), 122–129.

Cheng, L., Xu, Z.X., Wang, D.B., Cai, X.M., 2011. Assessing interannual variability of evapotranspiration at the catchment scale using satellite-based evapotranspiration data sets. Water Resour. Res. 47.

Choudhury, B.J., 1999. Evaluation of an empirical equation for annual evaporation using field observations and results from a biophysical model. J. Hydrol. 216 (1–2), 99–110.

Collins, D.B.G., Bras, R.L., 2007. Plant rooting strategies in water-limited ecosystems. Water Resour. Res. 43 (6).

Creed, I.F., et al., 2014. Changing forest water yields in response to climate warming: results from long-term experimental watershed sites across North America. Glob. Chang. Biol. 20 (10), 3191–3208.

de Boer-Euser, T., McMillan, H.K., Hrachowitz, M., Winsemius, H.C., Savenije, H.H.G., 2016. Influence of soil and climate on root zone storage capacity. Water Resour. Res. 52 (3), 2009–2024.

del Jesus, M., Foti, R., Rinaldo, A., Rodriguez-Iturbe, I., 2012. Maximum entropy production, carbon assimilation, and the spatial organization of vegetation in river basins. P Nat. Acad. Sci. USA 109 (51), 20837–20841.

Donohue, R.J., Roderick, M.L., McVicar, T.R., 2007. On the importance of including vegetation dynamics in Budyko's hydrological model. Hydrol. Earth Syst. Sc 11 (2), 983–995.

Donohue, R.J., Roderick, M.L., McVicar, T.R., 2012. Roots, storms and soil pores: Incorporating key ecohydrological processes into Budyko's hydrological model. J. Hydrol. 436, 35–50.

Donohue, R.J., Roderick, M.L., McVicar, T.R., Farquhar, G.D., 2013. Impact of CO2 fertilization on maximum foliage cover across the globe's warm, arid environments. Geophys. Res. Lett. 40 (12), 3031–3035.

Donohue, R.J., Roderick, M.L., McVicar, T.R., Yang, Y.T., 2017. A simple hypothesis of how leaf and canopy-level transpiration and assimilation respond to elevated CO2 reveals distinct response patterns between disturbed and undisturbed vegetation. J. Geophys. Res-Biogeo 122 (1), 168–184.

Dooge, J.C.I., Bruen, M., Parmentier, B., 1999. A simple model for estimating the sensitivity of runoff to long-term changes in precipitation without a change in vegetation. Adv. Water Resour. 23 (2), 153–163.

Du, C., Sun, F., Yu, J., Liu, X., Chen, Y., 2016. New interpretation of the role of water balance in an extended Budyko hypothesis in arid regions. Hydrol. Earth Syst. Sc 20 (1), 393–409.

Duan, Q., et al., 2006. Model Parameter Estimation Experiment (MOPEX): an overview of science strategy and major results from the second and third workshops. J. Hydrol. 320 (1–2), 3–17.

Eagleson, P.S., 1978a. Climate, soil, and vegetation. 1. Introduction to water-balance dynamics. Water Resour. Res. 14 (5), 705–712.

Eagleson, P.S., 1978b. Climate, soil, and vegetation. 4. Expected value of annual evapotranspiration. Water Resour. Res. 14 (5), 731–739.

Eagleson, P.S., 1982. Ecological optimality in water-limited natural soil-vegetation systems. 1. Theory and hypothesis. Water Resour. Res. 18 (2), 325–340.

Ellis, T., Hatton, T., Nuberg, I., 2005. An ecological optimality approach for predicting deep drainage from tree belts of alley farms in water-limited environments. Agr. Water Manag. 75 (2), 92–116.

Fang, K., Shen, C., Fisher, J.B., Niu, J., 2016. Improving Budyko curve-based estimates of long-term water partitioning using hydrologic signatures from GRACE. Water Resour. Res. 52 (7), 5537–5554.

Farquhar, G.D., Sharkey, T.D., 1982. Stomatal conductance and photosynthesis. Annu. Rev. Plant Physiol. 33 (33), 317–345.

Feng, X., Vico, G., Porporato, A., 2012. On the effects of seasonality on soil water balance and plant growth. Water Resour. Res. 48.

Field, C.B., Chapin, F.S., Matson, P.A., Mooney, H.A., 1992. Responses of terrestrial ecosystems to the changing atmosphere - a resource-based approach. Annu. Rev. Ecol. Syst. 23, 201–235.

Fu, B.P., 1981. On the calculation of evaporation from land surface (in Chinese). Sci. Atmos. Sin. 5, 23–31.

Gan, G.J., Gao, Y.C., 2015. Estimating time series of land surface energy fluxes using optimized two source energy balance schemes: model formulation, calibration, and validation. Agric. For. Meteorol. 208, 62–75.

Harman, C., Troch, P.A., 2020. Inferring transpiration from evapotranspiration: A transpiration indicator using the Priestley-Taylor coefficient of wet environment. Ecol Indic 110, 105853.

Gan, G., et al., 2019. An optimized two source energy balance model based on complementary concept and canopy conductance. Remote Sens. Environ. 223, 243–256.

Gao, G.Y., Fu, B.J., Wang, S., Liang, W., Jiang, X.H., 2016a. Determining the hydrological responses to climate variability and land use/cover change in the Loess Plateau with the Budyko framework. Sci. Total Environ. 557, 331–342.

Gao, Y.C., Gan, G.J., Liu, M.F., Wang, J.F., 2016b. Evaluating soil evaporation parameterizations at near-instantaneous scales using surface dryness indices. J. Hydrol. 541, 1199–1211.

Gentine, P., D'Odorico, P., Lintner, B.R., Sivandran, G., Salvucci, G., 2012. Interdependence of climate, soil, and vegetation as constrained by the Budyko curve. Geophys. Res. Lett. 39.

Gerrits, A.M.J., Savenije, H.H.G., Veling, E.J.M., Pfister, L., 2009. Analytical derivation of the Budyko curve based on rainfall characteristics and a simple evaporation model. Water Resour. Res. 45.

Gibson, J.J., Edwards, T.W.D., 2002. Regional water balance trends and evaporation-transpiration partitioning from a stable isotope survey of lakes in northern Canada. Glob. Biogeochem. Cy 16 (2).

Gnann, S.J., Woods, R.A., Howden, N.J.K., 2019. Is there a baseflow Budyko Curve? Water Resour. Res. 55 (4), 2838–2855.

Guswa, A.J., 2008. The influence of climate on root depth: a carbon cost-benefit analysis. Water Resour. Res. 44 (2).

Hall, A.E., Schulze, E.D., 1980. Stomatal response to environment and a possible interrelation between stomatal effects on transpiration and CO2 assimilation. Plant Cell Environ. 3 (6), 467–474.

Harman, C., Troch, P.A., 2014. What makes Darwinian hydrology "Darwinian"? Asking a different kind of question about landscapes. Hydrol Earth Syst Sc 18(2), 417–433.

Haughton, N., Abramowitz, G., De Kauwe, M.G., Pitman, A.J., 2018. Does predictability of fluxes vary between FLUXNET sites? Biogeosciences 15 (14), 4495–4513.

Helman, D., Lensky, I.M., Yakir, D., Osem, Y., 2017. Forests growing under dry conditions have higher hydrological resilience to drought than do more humid forests. Glob. Chang. Biol. 23 (7), 2801–2817.

Hibbert, A.R., 1967. Forest treatment effects on water yield. In: Sopper, W.E., Lull, H.W. (Eds.), Forest Hydrology, Proceedings of a National Science Foundation Advanced Science Seminar. Pergamon Press, Oxford, pp. 527–543.

Jaramillo, F., et al., 2018. Dominant effect of increasing forest biomass on evapotranspiration: interpretations of movement in Budyko space. Hydrol. Earth Syst. Sc 22 (1), 567–580.

Jiang, D., et al., 2014. The review of GRACE data applications in terrestrial hydrology monitoring. Adv. Meteorol., 725131

Jiang, C., et al., 2015. Separating the impacts of climate change and human activities on runoff using the Budyko-type equations with time-varying parameters. J. Hydrol. 522, 326–338.

Kleidon, A., Heimann, M., 1998. A method of determining rooting depth from a terrestrial biosphere model and its impacts on the global water and carbon cycle. Glob. Chang. Biol. 4 (3), 275–286.

Kokkonen, T.S., Jakeman, A.J., 2001. A comparison of metric and conceptual approaches in rainfall-runoff modeling and its implications. Water Resour. Res. 37 (9), 2345–2352.

Koster, R.D., Suarez, M.J., 1999. A simple framework for examining the interannual variability of land surface moisture fluxes. J. Clim. 12 (7), 1911–1917.

Kustas, W.P., Zhan, X.W., Jackson, T.J., 1999. Mapping surface energy flux partitioning at large scales with optical and microwave remote sensing data from Washita '92. Water Resour. Res. 35 (1), 265–277.

Leblanc, M.J., Tregoning, P., Ramillien, G., Tweed, S.O., Fakes, A., 2009. Basin-scale, integrated observations of the early 21st century multiyear drought in Southeast Australia. Water Resour. Res. 45.

Lei, H., Yang, D., Huang, M., 2014. Impacts of climate change and vegetation dynamics on runoff in the mountainous region of the Haihe River basin in the past five decades. J. Hydrol. 511 (4), 786–799.

Li, H.Y., Zhang, Y.Q., Vaze, J., Wang, B.D., 2012. Separating effects of vegetation change and climate variability using hydrological modelling and sensitivity-based approaches. J. Hydrol. 420, 403–418.

Li, D., Pan, M., Cong, Z.T., Zhang, L., Wood, E., 2013. Vegetation control on water and energy balance within the Budyko framework. Water Resour. Res. 49 (2), 969–976.
Li, H.Y., Sivapalan, M., Tian, F.Q., Harman, C., 2014. Functional approach to exploring climatic and landscape controls of runoff generation: 1. Behavioral constraints on runoff volume. Water Resour. Res. 50 (12), 9300–9322.
Li, C.B., et al., 2018. An analytical approach to separate climate and human contributions to basin streamflow variability. J. Hydrol. 559, 30–42.
Liang, W., et al., 2015. Quantifying the impacts of climate change and ecological restoration on streamflow changes based on a Budyko hydrological model in China's Loess Plateau. Water Resour. Res. 51 (8), 6500–6519.
Lima, L.S., et al., 2014. Feedbacks between deforestation, climate, and hydrology in the Southwestern Amazon: implications for the provision of ecosystem services. Landsc. Ecol. 29 (2), 261–274.
Liu, H.J., Cohen, S., Lemcoff, J.H., Israeli, Y., Tanny, J., 2015. Sap flow, canopy conductance and microclimate in a banana screenhouse. Agric. For. Meteorol. 201, 165–175.
Liu, J.Y., Zhang, Q., Singh, V.P., Shi, P.J., 2017. Contribution of multiple climatic variables and human activities to streamflow changes across China. J. Hydrol. 545, 145–162.
Liu, J.Y., et al., 2018. Hydrological effects of climate variability and vegetation dynamics on annual fluvial water balance in global large river basins. Hydrol. Earth Syst. Sc 22 (7), 4047–4060.
Liu, N., Harper, R.J., Smettem, K.R.J., Dell, B., Liu, S., 2019. Responses of streamflow to vegetation and climate change in southwestern Australia. J. Hydrol. 572, 761–770.
Long, D., et al., 2015. Deriving scaling factors using a global hydrological model to restore GRACE total water storage changes for China's Yangtze River Basin. Remote Sens. Environ. 168, 177–193.
Ma, Z.M., Kang, S.Z., Zhang, L., Tong, L., Su, X.L., 2008. Analysis of impacts of climate variability and human activity on streamflow for a river basin in arid region of Northwest China. J. Hydrol. 352 (3–4), 239–249.
Mao, D.Z., Cherkauer, K.A., 2009. Impacts of land-use change on hydrologic responses in the Great Lakes region. J. Hydrol. 374 (1–2), 71–82.
McVicar, T.R., et al., 2007. Developing a decision support tool for China's re-vegetation program: simulating regional impacts of afforestation on average annual streamflow in the Loess Plateau. Forest Ecol. Manag. 251 (1–2), 65–81.
Milly, P.C.D., 1993. An analytic solution of the stochastic storage problem applicable to soil-water. Water Resour. Res. 29 (11), 3755–3758.
Milly, P.C.D., 1994. Climate, soil-water storage, and the average annual water-balance. Water Resour. Res. 30 (7), 2143–2156.
Milly, P.C.D., et al., 2008. Climate change - Stationarity is dead: whither water management? Science 319 (5863), 573–574.
Monserud, R.A., Tchebakova, N.M., Leemans, R., 1993. Global vegetation change predicted by the modified Budyko model. Clim. Chang. 25 (1), 59–83.
Mu, Q.Z., Zhao, M.S., Running, S.W., 2011. Improvements to a MODIS global terrestrial evapotranspiration algorithm. Remote Sens. Environ. 115 (8), 1781–1800.
Murray, S.J., Foster, P.N., Prentice, I.C., 2012. Future global water resources with respect to climate change and water withdrawals as estimated by a dynamic global vegetation model. J. Hydrol. 448-449 (15), 14–29.
Nemani, R.R., Running, S.W., 1989. Testing a theoretical climate soil leaf-area hydrologic equilibrium of forests using satellite data and ecosystem simulation. Agric. For. Meteorol. 44 (3–4), 245–260.
Nijzink, R., et al., 2016. The evolution of root-zone moisture capacities after deforestation: a step towards hydrological predictions under change? Hydrol. Earth Syst. Sc 20 (12), 4775–4799.
Ning, T.T., Li, Z., Liu, W.Z., 2017. Vegetation dynamics and climate seasonality jointly control the interannual catchment water balance in the Loess Plateau under the Budyko framework. Hydrol. Earth Syst. Sc 21 (3), 1515–1526.
O'Grady, A.P., Carter, J.L., Bruce, J., 2011. Can we predict groundwater discharge from terrestrial ecosystems using existing eco-hydrological concepts? Hydrol. Earth Syst. Sc 15 (12), 3731–3739.
Ol'Dekop, E., 1911. On evaporation from the surface of river basins. Trans. Meteorol. Observ. 4.
Oudin, L., Andreassian, V., Lerat, J., Michel, C., 2008. Has land cover a significant impact on mean annual streamflow? An international assessment using 1508 catchments. J. Hydrol. 357 (3–4), 303–316.
Park, T., et al., 2016. Changes in growing season duration and productivity of northern vegetation inferred from long-term remote sensing data. Environ. Res. Lett. 11 (8).
Pate, J.S., Bell, T.L., 1999. Application of the ecosystem mimic concept to the species-rich Banksia woodlands of Western Australia. Agrofor. Syst. 45 (1–3), 303–341.
Penman, H.L., 1948. Natural evaporation from open water, bare soil and grass. Proc. R Soc. Lon. Ser-A 193 (1032), 120.
Pike, J.G., 1964. The estimation of annual run-off from meteorological data in a tropical climate. J. Hydrol. 2 (2), 116–123.
Porporato, A., Daly, E., Rodriguez-Iturbe, I., 2004. Soil water balance and ecosystem response to climate change. Am. Nat. 164 (5), 625–632.
Potter, N.J., Zhang, L., Milly, P.C.D., McMahon, T.A., Jakeman, A.J., 2005. Effects of rainfall seasonality and soil moisture capacity on mean annual water balance for Australian catchments. Water Resour. Res. 41 (6).
Priestley, C.H.B., Taylor, R.J., 1972. Assessment of surface heat-flux and evaporation using large-scale parameters. Mon. Weather Rev. 100 (2) (81−+).
Raupach, M.R., 2005. Dynamics and optimality in coupled terrestrial energy, water, carbon and nutrient cycles. Iahs-Aish P 301, 223–238.
Roderick, M.L., Farquhar, G.D., 2011. A simple framework for relating variations in runoff to variations in climatic conditions and catchment properties. Water Resour. Res. 47.
Rodriguez-Iturbe, I., 2000. Ecohydrology: a hydrologic perspective of climate-soil-vegetation dynamics. Water Resour. Res. 36 (1), 3–9.
Saft, M., Western, A.W., Zhang, L., Peel, M.C., Potter, N.J., 2015. The influence of multiyear drought on the annual rainfall-runoff relationship: an Australian perspective. Water Resour. Res. 51 (4), 2444–2463.
Saft, M., Peel, M.C., Western, A.W., Perraud, J.M., Zhang, L., 2016. Bias in streamflow projections due to climate-induced shifts in catchment response. Geophys. Res. Lett. 43 (4), 1574–1581.
Sankarasubramanian, A., Vogel, R.M., Limbrunner, J.F., 2001. Climate elasticity of streamflow in the United States. Water Resour. Res. 37 (6), 1771–1781.
Scanlon, T.M., Sahu, P., 2008. On the correlation structure of water vapor and carbon dioxide in the atmospheric surface layer: a basis for flux partitioning. Water Resour. Res. 44 (10).
Schenk, H.J., Jackson, R.B., 2002. The global biogeography of roots. Ecol. Monogr. 72 (3), 311–328.
Schewe, J., et al., 2014. Multimodel assessment of water scarcity under climate change. P Nat. Acad. Sci. USA 111 (9), 3245–3250.
Schreiber, P., 1904. Über die Beziehungen zwischen dem Niederschlag und der Wasserführung der Flüsse in Mitteleuropa. Z. Meteorol. 21, 441–452.
Schymanski, S.J., Sivapalan, M., Roderick, M.L., Hutley, L.B., Beringer, J., 2009. An optimality-based model of the dynamic feedbacks between natural vegetation and the water balance. Water Resour. Res. 45.
Schymanski, S.J., Roderick, M.L., Sivapalan, M., Hutley, L.B., Beringer, J., 2010. A test of the optimality approach to modelling canopy properties and CO2 uptake by natural vegetation.(vol 30, pg 1586, 2007). Plant Cell Environ. 33 (1), 130.
Shen, C., Jie, N., Phanikumar, M.S., 2013. Evaluating controls on coupled hydrologic and vegetation dynamics in a humid continental climate watershed using a subsurface-land surface processes model. Water Resour. Res. 49 (5), 2552–2572.
Shen, Q.N., Cong, Z.T., Lei, H.M., 2017. Evaluating the impact of climate and underlying surface change on runoff within the Budyko framework: a study across 224 catchments in China. J. Hydrol. 554, 251–262.
Sivapalan, M., 2006. Pattern, Process and Function: Elements of a Unified Theory of Hydrology at the Catchment Scale.
Sivapalan, M., Blöschl, G., Zhang, L., Vertessy, R., 2003. Downward Approach to Hydrological Prediction, 17, pp. 2101–2111.
Smettem, K., Callow, N., 2014. Impact of forest cover and aridity on the interplay between effective rooting depth and annual runoff in South-West Western Australia. Water-Sui 6 (9), 2539–2551.
Song, L.S., et al., 2018. Monitoring and validating spatially and temporally continuous daily evaporation and transpiration at river basin scale. Remote Sens. Environ. 219, 72–88.
Sposito, G., 2017. Understanding the Budyko equation. Water-Sui 9 (4).
Stednick, J.D., 1996. Monitoring the effects of timber harvest on annual water yield. J. Hydrol. 176 (1–4), 79–95.
Sun, G., Vose, J.M., 2016. Forest management challenges for sustaining water resources in the anthropocene. Forests 7 (3).
Sun, G., et al., 2005. Regional annual water yield from forest lands and its response to potential deforestation across the southeastern United States. J. Hydrol. 308 (1–4), 258–268.
Sun, G., et al., 2006. Potential water yield reduction due to forestation across China. J. Hydrol. 328 (3–4), 548–558.
Sun, G., Caldwell, P.V., McNulty, S.G., 2015. Modelling the potential role of forest thinning in maintaining water supplies under a changing climate across the conterminous United States. Hydrol. Process. 29 (24), 5016–5030.
Tang, Y., et al., 2017. Reconstructing annual groundwater storage changes in a large-scale irrigation region using GRACE data and Budyko model. J. Hydrol. 551, 397–406.
Troch, P.A., et al., 2009. Climate and vegetation water use efficiency at catchment scales. Hydrol. Process. 23 (16), 2409–2414.
Troch, P.A., Carrillo, G., Sivapalan, M., Wagener, T., Sawicz, K., 2013. Climate-vegetation-soil interactions and long-term hydrologic partitioning: signatures of catchment co-evolution. Hydrol. Earth Syst. Sc 17 (6), 2209–2217.
Troch, P.A., et al., 2015. Catchment coevolution: a useful framework for improving predictions of hydrological change? Water Resour. Res. 51 (7), 4903–4922.
Turc, L., 1954. The water balance of soils. Relation between precipitation, evaporation and flow. Annal. Agr. 5, 491–569.
van der Velde, Y., et al., 2014. Exploring hydroclimatic change disparity via the Budyko framework. Hydrol. Process. 28 (13), 4110–4118.
Van Dijk, A.U.M., Hairsine, P.B., Pena Arancibia, J., Dowling, T.I., 2007. Reforestation, water availability and stream salinity: a multi-scale analysis in the Murray-Darling Basin, Australia. Forest Ecol. Manag. 251 (1–2), 94–109.
van Wijk, M.T., Bouten, W., 2001. Towards understanding tree root profiles: simulating hydrologically optimal strategies for root distribution. Hydrol. Earth Syst. Sc 5 (4), 629–644.
Vickers, H., et al., 2016. Changes in greening in the high Arctic: insights from a 30 year AVHRR max NDVI dataset for Svalbard. Environ. Res. Lett. 11 (10).
Voepel, H., et al., 2011. Quantifying the role of climate and landscape characteristics on hydrologic partitioning and vegetation response. Water Resour. Res. 47.
Wan, Z.M., et al., 2015. Water balance-based actual evapotranspiration reconstruction from ground and satellite observations over the conterminous United States. Water Resour. Res. 51 (8), 6485–6499.
Wang, D.B., 2012. Evaluating interannual water storage changes at watersheds in Illinois based on long-term soil moisture and groundwater level data. Water Resour. Res. 48.
Wang, D.B., Hejazi, M., 2011. Quantifying the relative contribution of the climate and direct human impacts on mean annual streamflow in the contiguous United States. Water Resour. Res. 47.

Wang, D.B., Tang, Y., 2014. A one-parameter Budyko model for water balance captures emergent behavior in darwinian hydrologic models. Geophys. Res. Lett. 41 (13), 4569–4577.
Wang, X.S., Zhou, Y.X., 2016. Shift of annual water balance in the Budyko space for catchments with groundwater-dependent evapotranspiration. Hydrol. Earth Syst. Sc 20 (9), 3673–3690.
Wang, T.J., Istanbulluoglu, E., Lenters, J., Scott, D., 2009. On the role of groundwater and soil texture in the regional water balance: an investigation of the Nebraska Sand Hills, USA. Water Resour. Res. 45.
Wang, C., Wang, S., Fu, B.J., Zhang, L., 2016. Advances in hydrological modelling with the Budyko framework: a review. Prog. Phys. Geogr. 40 (3), 409–430.
Wang, T.T., et al., 2018. The predictability of annual evapotranspiration and runoff in humid and nonhumid catchments over China: comparison and quantification. J. Hydrometeorol. 19 (3), 533–545.
Warren, S.G., Schneider, S.H., 1979. Seasonal simulation as a test for uncertainties in the parameterizations of a Budyko-Sellers Zonal climate model. J. Atmos. Sci. 36 (8), 1377–1391.
Wei, X.H., et al., 2018. Vegetation cover-another dominant factor in determining global water resources in forested regions. Glob. Chang. Biol. 24 (2), 786–795.
Wiekenkamp, I., et al., 2016. Changes in measured spatiotemporal patterns of hydrological response after partial deforestation in a headwater catchment. J. Hydrol. 542, 648–661.
Williams, C.A., et al., 2012. Climate and vegetation controls on the surface water balance: Synthesis of evapotranspiration measured across a global network of flux towers. Water Resour. Res. 48.
Woods, R., 2003. The relative roles of climate, soil, vegetation and topography in determining seasonal and long-term catchment dynamics. Adv. Water Resour. 26 (3), 295–309.
Woodward, C., Shulmeister, J., Larsen, J., Jacobsen, G.E., Zawadzki, A., 2014. Landscape hydrology. The hydrological legacy of deforestation on global wetlands. Science 346 (6211), 844.
Xing, W.Q., Wang, W.G., Shao, Q.X., Yong, B., 2018a. Identification of dominant interactions between climatic seasonality, catchment characteristics and agricultural activities on Budyko-type equation parameter estimation. J. Hydrol. 556, 585–599.
Xing, W.Q., et al., 2018b. Estimating monthly evapotranspiration by assimilating remotely sensed water storage data into the extended Budyko framework across different climatic regions. J. Hydrol. 567, 684–695.
Xing, W.Q., Wang, W.G., Zou, S., Deng, C., 2018c. Projection of future runoff change using climate elasticity method derived from Budyko framework in major basins across China. Glob. Planet. Chang. 162, 120–135.
Xu, X.L., Liu, W., Scanlon, B.R., Zhang, L., Pan, M., 2013. Local and global factors controlling water-energy balances within the Budyko framework. Geophys. Res. Lett. 40 (23), 6123–6129.
Xu, X.Y., Yang, D.W., Yang, H.B., Lei, H.M., 2014. Attribution analysis based on the Budyko hypothesis for detecting the dominant cause of runoff decline in Haihe basin. J. Hydrol. 510, 530–540.
Yang, H.B., Yang, D.W., Lei, Z.D., Sun, F.B., 2008. New analytical derivation of the mean annual water-energy balance equation. Water Resour. Res. 44 (3).
Yang, D.W., et al., 2009. Impact of vegetation coverage on regional water balance in the nonhumid regions of China. Water Resour. Res. 45.
Yang, Y.T., Donohue, R.J., McVicar, T.R., 2016. Global estimation of effective plant rooting depth: Implications for hydrological modeling. Water Resour. Res. 52 (10), 8260–8276.
Ye, X.C., Zhang, Q., Liu, J., Li, X.H., Xu, C.Y., 2013. Distinguishing the relative impacts of climate change and human activities on variation of streamflow in the Poyang Lake catchment, China. J. Hydrol. 494, 83–95.
Ye, S., et al., 2015. Vegetation regulation on streamflow intra-annual variability through adaption to climate variations. Geophys. Res. Lett. 42 (23), 10307–10315.
Yokoo, Y., Sivapalan, M., Oki, T., 2008. Investigating the roles of climate seasonality and landscape characteristics on mean annual and monthly water balances. J. Hydrol. 357 (3–4), 255–269.
Zeng, R.J., Cai, X.M., 2015. Assessing the temporal variance of evapotranspiration considering climate and catchment storage factors. Adv. Water Resour. 79, 51–60.
Zeng, R.J., Cai, X.M., 2016. Climatic and terrestrial storage control on evapotranspiration temporal variability: analysis of river basins around the world. Geophys. Res. Lett. 43 (1), 185–195.
Zhang, L., Dawes, W.R., Walker, G.R., 2001. Response of mean annual evapotranspiration to vegetation changes at catchment scale. Water Resour. Res. 37 (3), 701–708.
Zhang, L., et al., 2004. A rational function approach for estimating mean annual evapotranspiration. Water Resour. Res. 40 (2).
Zhang, L., Potter, N., Hickel, K., Zhang, Y.Q., Shao, Q.X., 2008a. Water balance modeling over variable time scales based on the Budyko framework - Model development and testing. J. Hydrol. 360 (1–4), 117–131.
Zhang, X.P., et al., 2008b. Modelling the impact of afforestation on average annual streamflow in the Loess Plateau, China. Hydrol. Process. 22 (12), 1996–2004.
Zhang, Y.Q., et al., 2010. Using long-term water balances to parameterize surface conductances and calculate evaporation at 0.05 degrees spatial resolution. Water Resour. Res. 46.
Zhang, S.L., Yang, H.B., Yang, D.W., Jayawardena, A.W., 2016a. Quantifying the effect of vegetation change on the regional water balance within the Budyko framework. Geophys. Res. Lett. 43 (3), 1140–1148.
Zhang, Y.Q., et al., 2016b. Multi-decadal trends in global terrestrial evapotranspiration and its components. Sci. Rep-Uk 6.
Zhang, M.F., et al., 2017. A global review on hydrological responses to forest change across multiple spatial scales: Importance of scale, climate, forest type and hydrological regime. J. Hydrol. 546, 44–59.
Zhang, L., Cheng, L., Chiew, F., Fu, B.J., 2018a. Understanding the impacts of climate and landuse change on water yield. Curr. Opin. Environ. Sustain. 33, 167–174.
Zhang, S.L., Yang, Y.T., McVicar, T.R., Yang, D.W., 2018b. An analytical solution for the impact of vegetation changes on hydrological partitioning within the Budyko Framework. Water Resour. Res. 54 (1), 519–537.
Zhou, G.Y., et al., 2015. Global pattern for the effect of climate and land cover on water yield. Nat. Commun. 6.
Zhou, S., Yu, B.F., Zhang, Y., Huang, Y.F., Wang, G.Q., 2016. Partitioning evapotranspiration based on the concept of underlying water use efficiency. Water Resour. Res. 52 (2), 1160–1175.
Zhu, Z.C., et al., 2016. Greening of the Earth and its drivers. Nat. Clim. Chang. 6 (8) (791−+).